

Connection between Differential Geometry and Estimation Theory for Polynomial Nonlinearity in 2D

Mahendra Mallick

Georgia Tech Research Institute (GTRI)
Georgia Institute of Technology
Atlanta, GA 30332, U.S.A.
mahendra.mallick@gtri.gatech.edu

Sanjeev Arulampalam

Defence Science and Technology
Organisation
PO Box 1500, Edinburgh SA 5111, Australia
Sanjeev.Arulampalam@dsto.defence.gov.au

Yanjun Yan

Department of Electrical Engineering and
Computer Science, Syracuse University
Syracuse, NY 13244, U.S.A.
yayan@syr.edu

Aditya Mallick

Department of Mathematics
University of California at Los Angeles
Los Angeles, CA 90095, U.S.A.
amallick@ucla.edu

Abstract – *A relationship between differential geometry and estimation theory was lacking until the work of Bates and Watts in the context of nonlinear parameter estimation. They used differential geometry based curvature measures of nonlinearity (CMoN), namely, the parameter-effects and intrinsic curvatures to quantify the degree of nonlinearity of a general multi-dimensional nonlinear parameter estimation problem. However, they didn't establish a relationship between CMoN and the curvature in differential geometry. We consider a polynomial curve in two dimensions and for the first time show analytically and through Monte Carlo simulations that affine mappings with positive slopes exist among the logarithm of the curvature in differential geometry, Bates and Watts CMoN, and mean square error.*

Keywords: Differential Geometry, Extrinsic Curvature, Parameter-effects Curvature, Degree of Nonlinearity, Polynomial Nonlinearity, Curvature Measures of Nonlinearity, Mean Square Error, Cramér-Rao Lower Bound.

1 Introduction

Suppose we have a linear parameter estimation problem for a multi-dimensional non-random parameter with additive Gaussian measurement noise [1],[2]. Then the maximum likelihood (ML) estimate of the parameter can be calculated exactly and an exact analytic expression for the covariance of estimation error is possible [1],[2]. Exact confidence intervals for the components of the true parameter can be also calculated [2]. However, if the parameter estimation problem is nonlinear, then the parameter and the covariance of estimation error cannot be calculated exactly in all cases. A nonlinear parameter estimation algorithm commonly uses a linearization approximation or tangent plane approximation [3],[4] in the Taylor series expansion of the nonlinear measurement function about an estimate. If the tangent plane

approximation is valid, then the ML estimate is asymptotically unbiased, has asymptotic minimum mean square error (MMSE) (hence equal to the Cramér-Rao lower bound (CRLB) [5]), and is asymptotically normal [4]. However, if the tangent plane approximation is not valid, then these three asymptotic properties don't hold. Secondly, the confidence intervals for the true parameter are not accurate. For example, a 95% confidence intervals for a component of the true parameter does not contain the true value 95% of the time. The validity of the tangent plane approximation depends on the degree of nonlinearity [6, 7], [4].

Bates and Watts [6, 7] developed quantitative measures for the degree of nonlinearity of a nonlinear parameter estimation problem using differential geometry based CMoN, the parameter-effects and intrinsic curvatures. The parameter-effects curvature depends on the type of parameterization used for the nonlinear measurement function [3], [4]. Any nonlinear one-to-one mapping of the original parameter can change the parameter-effects curvatures. The intrinsic curvature is an intrinsic property of the nonlinear measurement function and does not depend on the type of parameterization used. Bates and Watts CMoN depend on the Jacobian and Hessian of the nonlinear function at an estimate and hence are random variables. Therefore, Bates and Watts curvatures show a great deal of variation with measurements, and the mean or median of the Bates and Watts curvature can be regarded as a curvature measure for the nonlinear estimation problem.

The curvature or more precisely the extrinsic curvature of curve in 2D at a point in the XY plane is a well known quantity in differential geometry [8], [9], [10]. The intrinsic curvature of such a curve is exactly zero. Similarly, the Gaussian and mean curvatures of a two-dimensional surface in 3D are also well known quantities [8]. The Gaussian and mean curvatures are intrinsic and extrinsic in nature, respectively. Extending these ideas to higher dimensions, we can

consider an n dimensional surface embedded in an m dimensional space, with $m > n$ and determine the extrinsic and intrinsic curvatures. These curvatures studied in differential geometry are non-random quantities.

We consider a curve in the XY plane with polynomial nonlinearity and estimate the x coordinate from noisy measurements of the y coordinate using single and multiple measurements. Then we calculate the extrinsic curvature $\kappa(x)$ [8], [9], [10], Bates and Watts parameter-effects curvature $K(\hat{x})$ [6, 7, 4], and direct parameter-effects curvature $\beta_\delta(\hat{x})$ [11, 12]. We derive expressions for the CRLB and expected values of the curvature measures analytically. If the MSE for the problem is close to the CRLB, then we can use the CRLB to study its dependence on the expected values of the curvature measures. Using Monte Carlo simulations, we also calculate the sample mean square error (SMSE), sample mean of $K(\hat{x})$ and $\beta_\delta(\hat{x})$. If the CMoN are to be meaningful measures for the degree of nonlinearity, then they should satisfy the following properties:

1. when the curvature measure increases, MSE increases,
2. when the curvature measure decreases, MSE decreases,
3. when the curvature measure is constant, so is MSE.

The above statements imply that the signs of the non-zero slopes of the curvature measure and MSE must be the same or both of them must have zero slopes. They should also hold when the CRLB is used in place of the MSE.

Our theoretical analyses and results from Monte Carlo simulations show the existence of the following affine mappings with positive slope parameters:

1. between $\log_{10} \text{MSE}(\hat{x})$ and $\log_{10} \mathbb{E}\{K(\hat{x})\}$,
2. between $\log_{10} \text{MSE}(\hat{x})$ and $\log_{10} \mathbb{E}\{\beta_\delta(\hat{x})\}$,
3. between $\log_{10} \mathbb{E}\{K(\hat{x})\}$ and $\log_{10} \kappa(x)$, and
4. between $\log_{10} \mathbb{E}\{\beta_\delta(\hat{x})\}$ and $\log_{10} \kappa(x)$.

Similar affine mappings are also shown using sample means by Monte Carlo simulations: the $\log_{10} \text{SMSE}$, $\log_{10} \bar{K}(\hat{x})$, and $\log_{10} \bar{\beta}_\delta(\hat{x})$.

A lower or upper case Roman or Greek italic letter represents a scalar and a lower or upper case bold Roman letter represents a vector or a matrix. We use the symbol “:=” to define a quantity.

The rest of the paper is organized as follows. We describe the extrinsic and parameter-effects curvatures for a curve in 2D in Section 2. In Section 3, we present a measurement model with polynomial nonlinearity and explain parameter estimation with single and multiple measurements, CRLB, extrinsic curvature, and parameter-effects curvatures. In Section 4, we first derive analytic expressions for the CRLB, mean of two parameter-effects curvatures, and then determine coefficients of various affine mappings analytically. We carry out Monte Carlo simulations in Section 5 to numerically evaluate the coefficients of various affine mappings, which are consistent with our analysis. Finally we present conclusions in Section 6.

2 Extrinsic and Parameter-effects Curvatures

2.1 Extrinsic Curvature of a Curve in 2D

Consider a curve in two dimensions. Intuitively, the curvature at a point determines the amount by which the curve deviates from a straight line. Thus a straight line has zero curvature at every point. The curvature of a circle at every point is equal to the inverse of the radius of the circle, which is a constant. A circle with a smaller radius bends more sharply and, therefore, has a higher curvature. The curvature of a smooth curve at a point is equal to the curvature of the osculating circle at that point. This curvature is known as the extrinsic curvature [10].

Consider a smooth curve in 2D

$$y = h(x), \quad (1)$$

where h is a nonlinear function whose first and second derivatives exist. The extrinsic curvature at the point x is defined by [8], [9],[10],

$$\kappa(x) := \frac{\left| \frac{d^2 h(x)}{dx^2} \right|}{\left[1 + \left(\frac{dh(x)}{dx} \right)^2 \right]^{3/2}} = \frac{|\ddot{h}(x)|}{\left[1 + \dot{h}(x)^2 \right]^{3/2}}. \quad (2)$$

2.2 Parameter-effects and Intrinsic Curvatures of a Curve in 2D

The parameter-effects and intrinsic curvatures defined by Bates and Watts [6, 7, 3, 4] are associated with an estimation problem and are defined at an estimate. We note that in (1), $h : \mathfrak{X} \rightarrow \mathfrak{R}$. Since the dimension of x and $\dot{y}(x)$ is unity, the intrinsic curvature of Bates and Watts $K_\delta^N(\hat{x})$ [6] or the direct intrinsic curvature $\beta_\delta^N(\hat{x})$ [11, 12] is zero. This is consistent with the zero intrinsic curvature from differential geometry. Thus only the parameter-effects curvature of Bates and Watts $K_\delta^T(\hat{x})$ and the direct parameter-effects curvature $\beta_\delta^T(\hat{x})$ exist and are given by

$$K(\hat{x}) := \frac{|\ddot{h}(\hat{x})\delta^2|}{|\dot{h}(\hat{x})\delta|^2} = \frac{|\ddot{h}(\hat{x})|\delta^2}{(\dot{h}(\hat{x}))^2\delta^2} = \frac{|\ddot{h}(\hat{x})|}{(\dot{h}(\hat{x}))^2}, \quad (3)$$

$$\beta_\delta(\hat{x}) := \frac{|\ddot{h}(\hat{x})\delta^2|}{|\dot{h}(\hat{x})\delta|} = \frac{|\ddot{h}(\hat{x})|\delta}{|\dot{h}(\hat{x})|}, \quad (4)$$

where

$$\delta := x - \hat{x}. \quad (5)$$

For simplicity in notation, we have dropped the superscript “T” in (3) and (4) since the intrinsic curvature is zero. Since K in (3) does not depend on δ we have also dropped the subscript from K in (3).

We note that the extrinsic curvature in (2) is evaluated at the true x , while the parameter-effects curvatures $K(\hat{x})$ in (3) and $\beta_\delta(\hat{x})$ in (4) are evaluated at the estimate \hat{x} . Therefore, $K(\hat{x})$ and $\beta_\delta(\hat{x})$ will depend on the type of estimator used. Since \hat{x} is a random variable, $K(\hat{x})$ and $\beta_\delta(\hat{x})$ are random variables. When we perform Monte Carlo simulations and

estimate x from measurements, \hat{x} will vary among Monte Carlo simulations. Therefore, $K(\hat{x})$ and $\beta_\delta(\hat{x})$ will vary over Monte Carlo simulations with certain distributions.

3 A Curve in 2D with Polynomial Nonlinearity

3.1 Measurement Model

We assume that the independent variable x is non-random. Suppose for a given x , we have N independent identically distributed (iid) measurements $\{z_i\}_{i=1}^N$. Since x is a scalar, we can estimate x from a single scalar measurement z . However, if we have multiple measurements $\{z_i\}$, then we can improve the estimation accuracy of \hat{x} .

Suppose we have N measurements $z_i, i = 1, \dots, N$,

$$z_i = h(x) + v_i, \quad (6)$$

where h and v_i are the polynomial measurement function and zero-mean white Gaussian measurement noise with variance σ_v^2 , respectively,

$$h(x) = ax^n, \quad (7)$$

$$v_i \sim \mathcal{N}(0, \sigma_v^2). \quad (8)$$

We estimate x given $z_i, i = 1, \dots, N$. We need the first and second derivatives of the nonlinear function h to calculate the extrinsic curvature and parameter-effects curvature. From (7) we have

$$\dot{h}(x) = anx^{n-1}, \quad n = 2, 3, \dots \quad (9)$$

$$\ddot{h}(x) = an(n-1)x^{n-2}, \quad n = 2, 3, \dots \quad (10)$$

The CRLB σ_{cr}^2 for this estimation problem is

$$\sigma_{\text{cr}}^2 = \frac{\sigma_v^2}{N \left(\frac{dh}{dx}\right)^2}. \quad (11)$$

Substitution (9) in (11) gives

$$\sigma_{\text{cr}}^2 = \frac{\sigma_v^2}{Nn^2a^2x^{2n-2}}. \quad (12)$$

Our numerical results indicate that the MSE for the current problem is nearly equal to the CRLB. Therefore, we use the CRLB to approximate the MSE.

3.2 Estimation With Multiple Measurements

We can write the measurement model in a vector form for multiple measurements for a given x . Define

$$\mathbf{z} := [z_1 \quad z_2 \quad \dots \quad z_N]^T, \quad (13)$$

$$\mathbf{v} := [v_1 \quad v_2 \quad \dots \quad v_N]^T, \quad (14)$$

$$\mathbf{h}(x) := h(x) [1 \quad 1 \quad \dots \quad 1]^T. \quad (15)$$

Then the measurement model for multiple measurements is

$$\mathbf{z} = \mathbf{h}(x) + \mathbf{v}, \quad (16)$$

$$\mathbf{v} \sim N(\mathbf{0}, \mathbf{R}), \quad \mathbf{R} = I_N \sigma_v^2. \quad (17)$$

From (17)

$$\mathbf{R}^{-1} = I_N \sigma_v^{-2}, \quad |\mathbf{R}| = \sigma_v^{2N}. \quad (18)$$

Using (16)-(18), the likelihood function for x is

$$p(\mathbf{z}|x) = \frac{\exp\left[-\frac{1}{2\sigma_v^2}[(\mathbf{z} - \mathbf{h}(x))'(\mathbf{z} - \mathbf{h}(x))]\right]}{[(2\pi\sigma_v^2)^N]^{1/2}}. \quad (19)$$

From (19), we observe that the ML estimate of x is obtained by solving the nonlinear least squares (NLS) problem

$$\min_x (\mathbf{z} - \mathbf{h}(x))'(\mathbf{z} - \mathbf{h}(x)). \quad (20)$$

To solve the nonlinear optimization problem in (20), we need an initial estimate \hat{x}_1 of x , which can be derived using any single measurement, such as z_1 . An estimate of x using z_1 is given by

$$\hat{x}_1 = (z_1/a)^{1/n}, \quad n = 2, 3, \dots \quad (21)$$

3.3 Extrinsic Curvature

From (2), the extrinsic curvature for the problem is

$$\kappa(x) = \frac{|an(n-1)x^{n-2}|}{[1 + (anx^{n-1})^2]^{3/2}}, \quad n = 2, 3, \dots \quad (22)$$

3.4 Parameter-effects Curvatures

Using (9) and (10) in (3) and (4), we get the expressions for the Bates and Watts and direct parameter-effects curvatures $K(\hat{x})$ and $\beta_\delta(\hat{x})$, respectively,

$$K(\hat{x}) = \frac{(n-1)}{n|a||\hat{x}^n|}, \quad (23)$$

$$\beta_\delta(\hat{x}) = \frac{|an(n-1)\hat{x}^{n-2}\delta|}{|an\hat{x}^{n-1}|} = (n-1) \frac{|\delta|}{|\hat{x}|}. \quad (24)$$

4 Mapping between CMoN and MSE

The nonlinearity of the problem imposes challenges in parameter estimation. We analyze the CMoN and MSE of the nonlinear estimation problem to discover relationships among them. For the current problem, CMoN are measured by the parameter-effects curvature in (23) and the direct parameter-effects curvature in (24). In general, CMoN depend on the first and second derivatives of the nonlinear function calculated at the parameter estimate and on the norm of the estimation error for $\beta_\delta(\hat{x})$. Therefore, the CMoN will depend the type of estimator (e.g. ML) used to obtain parameter estimate. The extrinsic curvature (22) depend on the first and second derivatives of the nonlinear function evaluated at the true x .

4.1 MSE and SMSE

We estimate the x coordinate using noisy measurements at a discrete set $\{x_k\}_{k=1}^{N_x}$ of values. Let $\hat{x}_{k,m}$ denote the estimate of x_k in the m th Monte Carlo run. Then the error $\tilde{x}_{k,m}$ in $\hat{x}_{k,m}$ is defined by

$$\tilde{x}_{k,m} := x_k - \hat{x}_{k,m}, \quad k = 1, 2, \dots, N_x, \quad m = 1, 2, \dots, M, \quad (25)$$

where M is the number of Monte Carlo runs. The MSE at x_k is given by

$$\text{MSE}_k = \mathbb{E}\{(\tilde{x}_{k,m})^2\}, \quad k = 1, 2, \dots, N_x. \quad (26)$$

The SMSE at x_k is defined by

$$\text{SMSE}_k := \frac{1}{M} \sum_{m=1}^M (\tilde{x}_{k,m})^2, \quad k = 1, 2, \dots, N_x. \quad (27)$$

Let $L_{\text{cr}}(x)$ denote the \log_{10} of the CRLB,

$$L_{\text{cr}}(x) := \log_{10} \sigma_{\text{cr}}^2. \quad (28)$$

Taking the log of (12) we get

$$L_{\text{cr}}(x) = \log_{10} \left(\frac{\sigma_v^2}{Nn^2a^2} \right) - 2(n-1) \log_{10} x. \quad (29)$$

4.2 MSE and Parameter-effects Curvature

Let $L_K(x)$ denote the log of the expected value of $K(\hat{x})$ in (23). Then

$$L_K(x) := \log_{10} (\mathbb{E}(K(\hat{x}))). \quad (30)$$

In order to compute $L_K(x)$ we first approximate the expectation in (30) by assuming $\sigma_{\hat{x}} \ll x$, which holds for the case investigated in our paper,

$$\begin{aligned} \mathbb{E}[K(\hat{x})] &= \frac{(n-1)}{na} \mathbb{E} \left(\frac{1}{|\hat{x}^n|} \right) \\ &\approx \frac{(n-1)}{na} \frac{1}{(\mathbb{E}[|\hat{x}|])^n} \\ &\approx \frac{(n-1)}{na} \frac{1}{x^n}. \end{aligned} \quad (31)$$

The last step of the above equation follows from an assumption that the estimator is nearly unbiased. Now, taking the logarithm we have

$$L_K(x) = \log_{10} \left(\frac{n-1}{na} \right) - n \log_{10} x. \quad (32)$$

Now from equations (32) and (29) we can see that there is an affine mapping between $L_{\text{cr}}(x)$ and $L_K(x)$. That is,

$$L_{\text{cr}}(x) = \alpha_1^K L_K(x) + \alpha_0^K, \quad (33)$$

where

$$\begin{aligned} \alpha_1^K &= \frac{2(n-1)}{n}, \\ \alpha_0^K &= \log_{10} \left(\frac{\sigma_v^2}{Nn^2a^2} \right) - \frac{2(n-1)}{n} \log_{10} \left(\frac{n-1}{na} \right). \end{aligned} \quad (34)$$

We observe that α_1^K is positive and hence $L_K(x)$ and $L_{\text{cr}}(x)$ have the same sign of the non-zero slopes. As a result, $K(\hat{x})$ and CRLB have the same sign of the non-zero slopes.

4.3 MSE and Direct Parameter-effects Curvature

The expression for the direct parameter-effects curvature $\beta_{\delta}(\hat{x})$ [11, 12] is given by (24). Similar to the previous section, we define

$$L_{\beta}(x) := \log_{10} (\mathbb{E}[\beta_{\delta}(\hat{x})]). \quad (35)$$

Now, taking the expected value of β we have

$$\begin{aligned} \mathbb{E}[\beta(\hat{x})] &\approx \frac{(n-1)}{x} \mathbb{E}[|\delta|] \\ &= \frac{(n-1)}{x} \mathbb{E}[|\hat{x} - x|]. \end{aligned} \quad (36)$$

The RHS of (36) can be simplified by assuming that \hat{x} is unbiased and that it achieves the CRLB. Also, we approximate this error to be Gaussian, i.e., we use

$$(\hat{x} - x) \sim \mathcal{N}(0, \sigma_{\text{cr}}^2). \quad (37)$$

Then,

$$\mathbb{E}[|\hat{x} - x|] = \sigma_{\text{cr}} \sqrt{\frac{2}{\pi}}. \quad (38)$$

Substituting (38) into (36) and using (12) for σ_{cr}^2 we have

$$\mathbb{E}[\beta(\hat{x})] \approx \frac{(n-1)}{na} \sigma_v \sqrt{\frac{2}{N\pi}} x^{-n}. \quad (39)$$

Thus,

$$L_{\beta}(x) \approx \log_{10} \left[\frac{(n-1) \sigma_v \sqrt{\frac{2}{N\pi}}}{na} \right] - n \log_{10} x. \quad (40)$$

From (40) and (29) we can write the affine mapping

$$L_{\text{cr}}(x) = \alpha_1^{\beta} L_{\beta}(x) + \alpha_0^{\beta}, \quad (41)$$

where

$$\begin{aligned} \alpha_1^{\beta} &= \frac{2(n-1)}{n}, \\ \alpha_0^{\beta} &= \log_{10} \left(\frac{\sigma_v^2}{Nn^2a^2} \right) - \frac{2n-2}{n} \log_{10} \left[\frac{(n-1) \sigma_v \sqrt{2}}{na \sqrt{N\pi}} \right]. \end{aligned} \quad (42)$$

We also observe that α_1^{β} is positive and hence $L_{\beta}(x)$ and $L_{\text{cr}}(x)$ have the same sign of the non-zero slopes. As a result, $\beta_{\delta}(\hat{x})$ and CRLB have the same sign of the non-zero slopes.

4.4 Extrinsic Curvature

The expression for extrinsic curvature for our problem is given in (22). Similar to previous sections, we define

$$L_E(x) := \log_{10} (\kappa(x)). \quad (43)$$

Taking the log of (43) we have

$$\begin{aligned}
L_E(x) &= \log_{10}(\kappa(x)) \\
&= \log_{10} [an(n-1)x^{n-2}] - \frac{3}{2} \log_{10} [1 + (anx^{n-1})^2] \\
&\approx \log_{10} [an(n-1)x^{n-2}] - \frac{3}{2} \log_{10} [(anx^{n-1})^2] \\
&= \log_{10} \left[\frac{n-1}{(an)^2} \right] - (2n-1) \log_{10} x. \tag{44}
\end{aligned}$$

Note that the second last expression is a valid approximation for $x > 2$. From (44) and (32) it is easy to establish the affine mapping

$$L_K(x) = \gamma_1^K L_E(x) + \gamma_0^K, \tag{45}$$

where

$$\begin{aligned}
\gamma_1^K &= \frac{n}{2n-1}, \\
\gamma_0^K &= \log_{10} \left(\frac{n-1}{na} \right) - \frac{n}{2n-1} \log_{10} \left[\frac{n-1}{(an)^2} \right] \tag{46}
\end{aligned}$$

Similarly, from (44) and (40) we can establish the affine relationship

$$L_\beta(x) = \gamma_1^\beta L_E(x) + \gamma_0^\beta, \tag{47}$$

where

$$\begin{aligned}
\gamma_1^\beta &= \frac{n}{2n-1}, \\
\gamma_0^\beta &= \log_{10} \left(\frac{(n-1)\sigma_v\sqrt{2}}{na\sqrt{N\pi}} \right) - \frac{n}{2n-1} \log_{10} \left[\frac{n-1}{(an)^2} \right]. \tag{48}
\end{aligned}$$

Using similar arguments used in previous sections, we infer that the extrinsic curvature and parameter-effects curvature have the same sign of the non-zero slopes. Similarly, the extrinsic curvature and direct parameter-effects curvature have the same non-zero slopes.

4.5 Estimation of CMoN and SMSE by Monte-Carlo Simulations

Let $\bar{K}(\hat{x}_k)$ and $\bar{\beta}_\delta(\hat{x}_k)$ denote the sample means of the Bates and Watts and direct parameter-effects curvatures calculated from M Monte Carlo runs. Then

$$\bar{K}(\hat{x}_k) := \frac{1}{M} \sum_{m=1}^M K(\hat{x}_{k,m}), \quad k = 1, 2, \dots, N_x, \tag{49}$$

$$\bar{\beta}_\delta(\hat{x}_k) := \frac{1}{M} \sum_{m=1}^M \beta_\delta(\hat{x}_{k,m}), \quad k = 1, 2, \dots, N_x. \tag{50}$$

Correspondingly, we define

$$b_k := \log_{10} \text{SMSE}_k, \quad k = 1, 2, \dots, N_x, \tag{51}$$

$$c_k := \log_{10} \bar{K}(\hat{x}_k), \quad k = 1, 2, \dots, N_x, \tag{52}$$

$$d_k := \log_{10} \bar{\beta}_\delta(\hat{x}_k), \quad k = 1, 2, \dots, N_x. \tag{53}$$

Define

$$\mathbf{b} := [b_1 \quad b_2 \quad \dots \quad b_{N_x}]', \tag{54}$$

$$\mathbf{c} := [c_1 \quad c_2 \quad \dots \quad c_{N_x}]', \tag{55}$$

$$\mathbf{d} := [d_1 \quad d_2 \quad \dots \quad d_{N_x}]'. \tag{56}$$

Suppose an affine mapping exists between \mathbf{b} and \mathbf{c} . Then

$$b_k = \hat{\alpha}_1^K c_k + \hat{\alpha}_0^K + e_k, \quad k = 1, 2, \dots, N_x, \tag{57}$$

where e_k is a random noise. Then we can write (57) in the matrix-vector form by

$$\mathbf{b} = \mathbf{H}_c \boldsymbol{\alpha} + \mathbf{e}, \tag{58}$$

where

$$\boldsymbol{\alpha} := [\hat{\alpha}_1^K \quad \hat{\alpha}_0^K]', \tag{59}$$

$$\mathbf{e} := [e_1 \quad e_2 \quad \dots \quad e_{N_x}]', \tag{60}$$

$$\mathbf{H}_c := \begin{bmatrix} c_1 & 1 \\ c_2 & 1 \\ \dots & \dots \\ c_{N_x} & 1 \end{bmatrix}. \tag{61}$$

Given \mathbf{b} and \mathbf{H}_c , we can estimate $\boldsymbol{\alpha}$ using the linear least squares (LLS).

We can similarly define the affine mapping between other variable pairs. Altogether we consider the following four:

1. between \mathbf{b} ($\log_{10}(\text{SMSE}_k)$) and \mathbf{c} ($\log_{10}(\bar{K}(\hat{x}_k))$) for each power of the polynomial function, as in (33),
2. between \mathbf{b} ($\log_{10}(\text{SMSE}_k)$) and \mathbf{d} ($\log_{10}(\bar{\beta}_\delta(\hat{x}_k))$) for each power of the polynomial function, as in (41),
3. between \mathbf{c} ($\log_{10}(\bar{K}(\hat{x}_k))$) and $\log_{10}(\kappa(x_k))$ (43) for each power of the polynomial function, as in (45), and
4. between \mathbf{d} ($\log_{10}(\bar{\beta}_\delta(\hat{x}_k))$) and $\log_{10}(\kappa(x_k))$ (43) for each power of the polynomial function, as in (47).

5 Numerical Simulation and Results

In the numerical simulations, we used $a = 0.6$ and $n = 2, 3, 4, 5$ and a number of uniformly spaced x coordinates with the spacing 0.1 in the interval $[2, 7]$. The measurement noise standard deviation σ was 0.5. Figure 1 illustrates $\log_{10}(y)$ versus x . Figure 2 shows the log of the extrinsic curvature $\log_{10}(\kappa(x))$ versus x . The extrinsic curvature is completely determined by the nonlinear function, and it is independent of parameter estimation.

5.1 Single Measurement Results

In this section, we use a single measurement z to estimate each x . The performance is analyzed using 1000 Monte Carlo simulations. The log of MSE is reported in Figure 3. The parameter-effects curvatures K for Monte-Carlo simulations is illustrated in Figure 4, which varies more when n and x are small. The direct parameter-effects curvatures β_δ for Monte-Carlo simulations is illustrated in Figure 5, which varies much more than K . Now that the data spread of β_δ for different power n overlaps in Figure 5, they are again plotted individually in Figure 6.

The simulated and theoretical affine mapping coefficients for the four pairs are provided in Table 1. The affine mapped

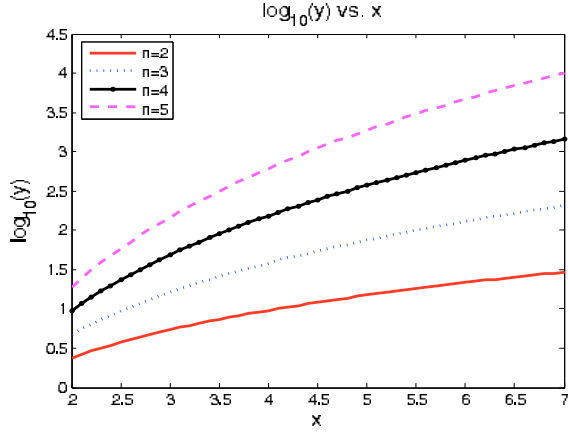


Figure 1: $\log_{10}(y)$ versus x for $x=2.0$ to 7.0 with a uniform interval of 0.1 .

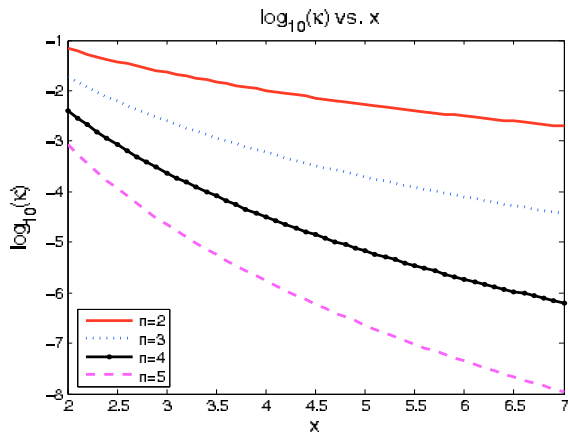


Figure 2: $\log_{10}(\kappa(x))$ versus x .

results are plotted in Figures 7-10. Figures 7-8 show the original $\log_{10}(\text{SMSE})$ from 1000 Monte Carlo runs and affine-mapped $\log_{10}(\text{SMSE})$ obtained from $\log_{10}(\bar{K}(\hat{x}))$ and $\log_{10}(\bar{\beta}_{\delta}(\hat{x}))$, respectively with *positive slopes* of the affine mappings as shown in Table 1. The original and affine mapped plots are very close to each other in Figures 7-8. Secondly, Figures 9-10 show the original $\log_{10}(\bar{K}(\hat{x}))$ and $\log_{10}(\bar{\beta}_{\delta}(\hat{x}))$ and corresponding affine-mapped values obtained from $\log_{10}(\kappa)$. Similarly, the original and affine mapped plots are very close to each other in Figures 9-10.

5.2 Multiple Measurements Results

In this section, we carry out experiments for N from 3 to 20, and the trend of the variation of the affine coefficients is consistent. Due to space limitation, we provide the results for $N = 3$ and $N = 20$. For $N = 3$, the affine mapping coefficients are provided in Table 2. For $N = 20$, the affine mapping coefficients are provided in Table 3.

6 Discussions and Conclusions

We have analyzed a curve in 2D with polynomial non-linearity and calculated the extrinsic curvatures, Bates and

Watts and direct parameter-effects curvatures, and MSE. Results from our theoretical analysis and Monte Carlo simulations show that there exists a number of excellent affine mappings with positive slopes among (i) $\log(\text{CMoN})$ and $\log(\text{SMSE})$ and (ii) $\log(\kappa)$ and $\log(\text{SMSE})$. The parameters of the affine mappings obtained from theoretical analysis agree well with those from Monte Carlo simulations as shown in Tables 1-3.

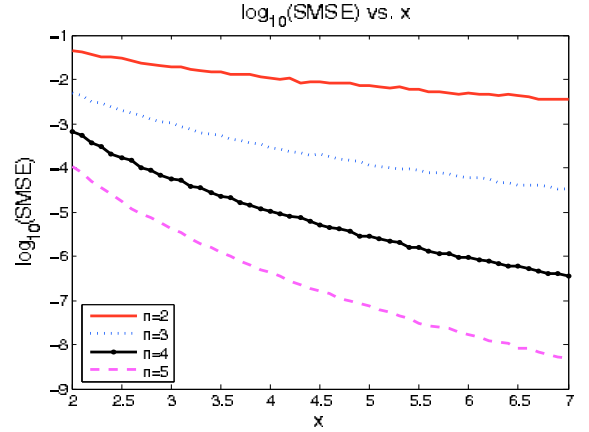


Figure 3: $\log_{10}(\text{SMSE})$ versus x .

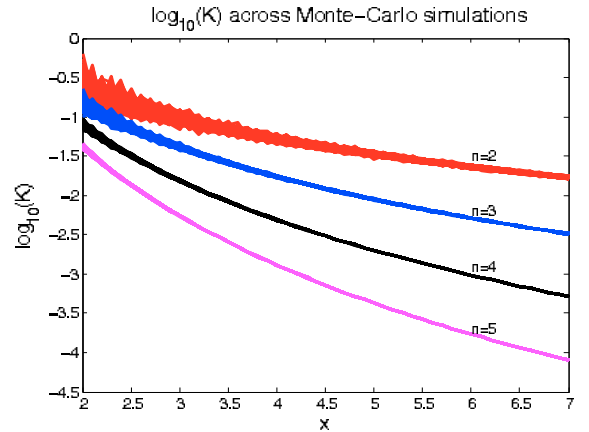


Figure 4: $\log_{10}K(\hat{x})$ versus x .

References

- [1] J. M. Mendel, *Lessons in Estimation Theory for Signal Processing Communications, and Control*, Prentice-Hall, 1995.
- [2] R. A. Johnson and D. W. Wichern, *Applied Multivariate Statistical Analysis*, Third Edition, Prentice-Hall, 1982.
- [3] D. M. Bates and D. G. Watts, *Nonlinear Regression Analysis and its Applications*, John Wiley, 1988.
- [4] G. A. Seber and C. J. Wild, *Nonlinear Regression*, John Wiley, 1989.

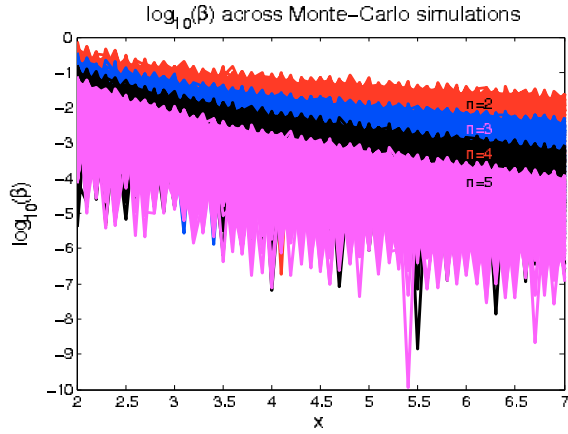


Figure 5: $\log_{10}(\beta_\delta(\hat{x}))$ versus x across Monte-Carlo simulations (The plots with different n 's are overlapped).

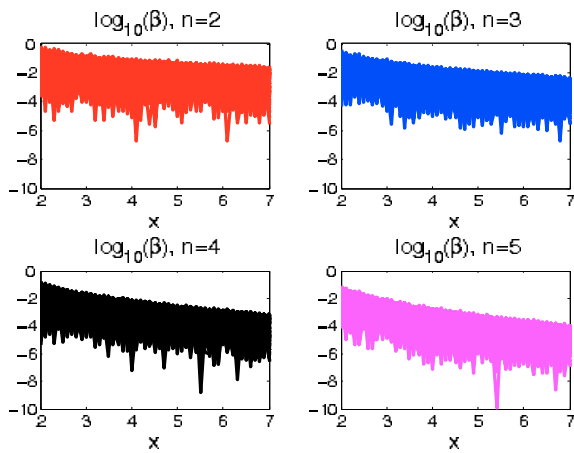


Figure 6: $\log_{10}\beta_\delta(\hat{x})$ versus x across Monte-Carlo simulations (Each subplot is with a different n).

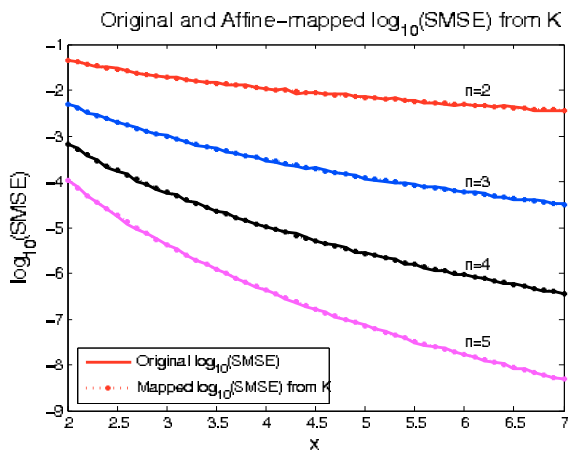


Figure 7: The original $\log_{10}(\text{SMSE})$ and the affine-mapped $\log_{10}(\text{SMSE})$ from $\log_{10}(\bar{K}(\hat{x}))$.

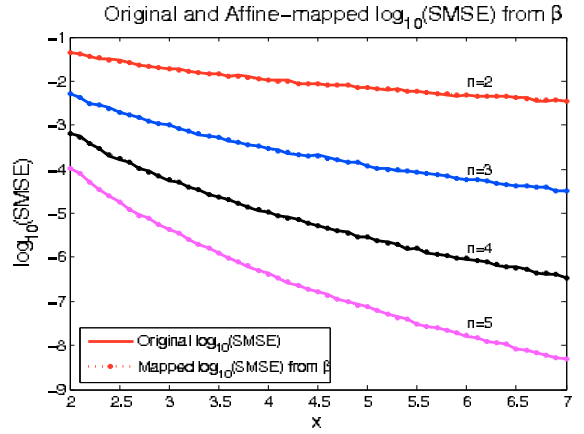


Figure 8: The original $\log_{10}(\text{SMSE})$ and the affine-mapped $\log_{10}(\text{SMSE})$ from $\log_{10}(\beta_\delta(\hat{x}))$.

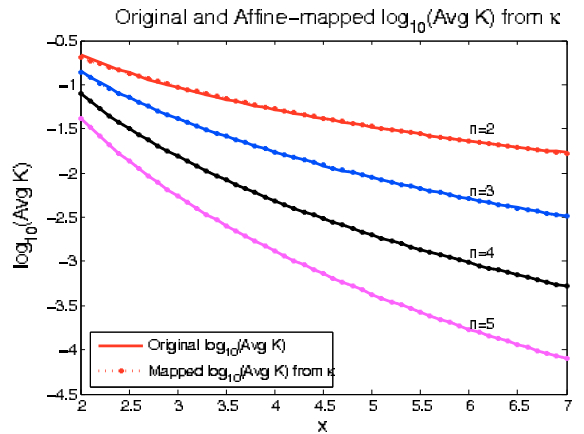


Figure 9: The original $\log_{10}(\bar{K}(\hat{x}))$ and the affine-mapped $\log_{10}(\bar{K}(\hat{x}))$ from $\log_{10}(\kappa(x))$.

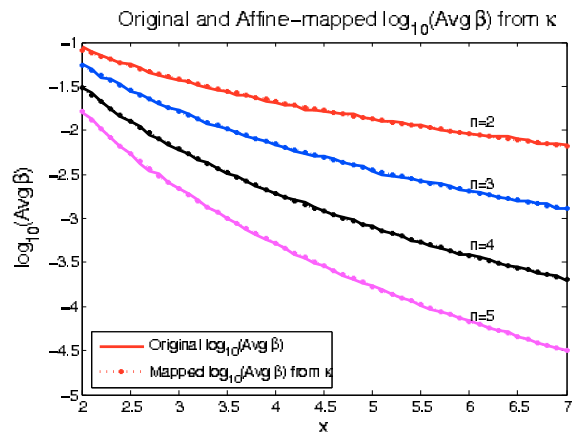


Figure 10: The original $\log_{10}(\bar{\beta}_\delta(\hat{x}))$ and the affine-mapped $\log_{10}(\bar{\beta}_\delta(\hat{x}))$ from $\log_{10}(\kappa(x))$.

[5] B. Ristic, S. Arulampalam, and N. Gordon, *Beyond the Kalman Filter*, Artech House, 2004.

[6] D. M. Bates and D. G. Watts, "Relative curvature mea-

asures of nonlinearity," *Journal of the Royal Statistical Society. Series B (Methodological)*, vol. 42, no. 1, pp. 1–25, 1980.

- [7] D. M. Bates, D. C. Hamilton, and D. G. Watts, "Calculation of intrinsic and parameter-effects curvatures for nonlinear regression models," *Communications in Statistics - Simulation and Computation*, vol. 12, no. 4, pp. 469–477, 1983.
- [8] M. Do Carmo, *Differential Geometry of Curves and Surfaces*, Prentice-Hall, 1976.
- [9] D. J. Struik, *Lectures on Classical Differential Geometry*, Dover Publications, 2 ed., 1988.
- [10] <http://en.wikipedia.org/wiki/curvature>.
- [11] M. Mallick, B. F. La Scala, and M. S. Arulampalam, "Differential geometry measures of nonlinearity for the bearing-only tracking problem," in *Proc. SPIE*, Vol. 5809, pp. 288–300, May 2005.
- [12] M. Mallick, B. F. L. Scala, and S. Arulampalam, "Differential geometry measures of nonlinearity with applications to target tracking," in *Fred Daum Tribute Conference*, (Monterey, California), May 2007.

Table 2: Comparison of affine mapping parameters: simulations and theory, multiple measurements ($N = 3$)

n	α_1^K (sim)	α_1^K (theory)	α_0^K (sim)	α_0^K (theory)
2	0.99674	1.0000	-1.1669	-1.1584
3	1.3215	1.3333	-1.6761	-1.6507
4	1.4974	1.5000	-1.989	-1.9850
5	1.6031	1.6000	-2.226	-2.2333
n	α_1^β (sim)	α_1^β (theory)	α_0^β (sim)	α_0^β (theory)
2	1.0006	1.0000	-0.52251	-0.52071
3	1.3299	1.3333	-0.81068	-0.80054
4	1.4985	1.5000	-1.0315	-1.0285
5	1.6005	1.6000	-1.2124	-1.2131
n	γ_1^K (sim)	γ_1^K (theory)	γ_0^K (sim)	γ_0^K (theory)
2	0.70386	0.66667	0.12543	0.026394
3	0.60207	0.60000	0.17957	0.17147
4	0.57163	0.57143	0.25986	0.25880
5	0.55557	0.55556	0.32070	0.32060
n	γ_1^β (sim)	γ_1^β (theory)	γ_0^β (sim)	γ_0^β (theory)
2	0.70169	0.66667	-0.51792	-0.61126
3	0.59837	0.60000	-0.47201	-0.46618
4	0.57121	0.57143	-0.37924	-0.37885
5	0.55649	0.55556	-0.31198	-0.31705

Table 1: Comparison of affine mapping parameters: simulations and theory, single measurement ($N = 1$)

n	α_1^K (sim)	α_1^K (theory)	α_0^K (sim)	α_0^K (theory)
2	0.9919	1.0000	-0.6929	-0.6812
3	1.3383	1.3333	-1.1641	-1.1736
4	1.5022	1.5000	-1.5107	-1.5078
5	1.5993	1.6000	-1.7618	-1.7562
n	α_1^β (sim)	α_1^β (theory)	α_0^β (sim)	α_0^β (theory)
2	0.9925	1.0000	-0.2978	-0.2822
3	1.3364	1.3333	-0.6347	-0.6415
4	1.5008	1.5000	-0.9084	-0.9092
5	1.5998	1.6000	-1.1178	-1.1177
n	γ_1^K (sim)	γ_1^K (theory)	γ_0^K (sim)	γ_0^K (theory)
2	0.7098	0.6667	0.1397	0.02639
3	0.6026	0.6000	0.1818	0.1715
4	0.5717	0.5714	0.2601	0.2588
5	0.5556	0.5556	0.3207	0.3206
n	γ_1^β (sim)	γ_1^β (theory)	γ_0^β (sim)	γ_0^β (theory)
2	0.7098	0.6667	-0.2577	-0.3727
3	0.6036	0.6000	-0.2139	-0.2276
4	0.5722	0.5714	-0.1409	-0.1403
5	0.5554	0.5556	-0.08195	-0.07849

Table 3: Comparison of affine mapping parameters: simulations and theory, multiple measurements ($N = 20$)

n	α_1^K (sim)	α_1^K (theory)	α_0^K (sim)	α_0^K (theory)
2	0.97594	1.000	-2.0113	-1.9823
3	1.3351	1.333	-2.4742	-2.4746
4	1.4989	1.500	-2.8088	-2.8089
5	1.5952	1.600	-3.0757	-3.0572
n	α_1^β (sim)	α_1^β (theory)	α_0^β (sim)	α_0^β (theory)
2	0.98855	1.000	-0.95794	-0.93267
3	1.3372	1.333	-1.0647	-1.0752
4	1.5015	1.500	-1.2291	-1.2345
5	1.5971	1.600	-1.3888	-1.3779
n	γ_1^K (sim)	γ_1^K (theory)	γ_0^K (sim)	γ_0^K (theory)
2	0.70188	0.66667	0.12059	0.026394
3	0.6018	0.60000	0.17853	0.17147
4	0.57156	0.57143	0.25951	0.2588
5	0.55557	0.55556	0.32067	0.3206
n	γ_1^β (sim)	γ_1^β (theory)	γ_0^β (sim)	γ_0^β (theory)
2	0.69331	0.66667	-0.94575	-1.0232
3	0.60098	0.60000	-0.87546	-0.87814
4	0.5706	0.57143	-0.79284	-0.79081
5	0.5549	0.55556	-0.73591	-0.72901